A Comparative Analysis of Detecting Bearing Fault, Using Infrared Thermography, Vibration Analysis and Air-Borne Sound

Nikolaos G. Athanasopoulos and Pantelis N. Botsaris

Abstract A comparative analysis has been performed as an effort to obtain a better idea of how the fault is appearing over a rolling bearing. In this paper are presented the results of this analysis between three methods of detecting faults on bearings: infrared thermography, vibration analysis and air-borne sound. Those methods are applied on a specific rolling bearing and developed on an experimental set up. The conducted experiment depicted that this comparison is feasible as the results of each method are relevant.

1 Introduction

Ball and rolling element bearings are perhaps the most widely used components in industrial machinery. They are used to support load and allow relative motion inherent in the mechanism to take place. Different methods are used for the detection and diagnosis of bearing defects; they may be broadly classified as vibration and acoustic measurements, temperature measurements and wear debris analysis [1].

N. G. Athanasopoulos (✉) · P. N. Botsaris
Democritus University of Thrace, School of Engineering, Department of Production Engineering and Management, Laboratory of Mechanical Design, 12 Vas. Sofias, Xanthi, Thrace-Hellas, Greece
e-mail: nikoatha@gmail.com

P. N. Botsaris
e-mail: panmpots@pme.duth.gr

The temperature is an important value measured to present the bearing fault. Measurements of the temperature are used in parallel with other parameters like vibration measurements for the detection of fault. The temperature of the bearings and the lubricant is an indication of the state of machine. Increased temperature in outer rings bearings warns for the initiation of the damage.

As regards the temperature of the lubricant is usually from 10 to 20 °C lower than the bearing. Most lubricants for each 15 °C increase in temperature over 70 °C, have their life halved (or even more), occurring negative effect on the life of the bearing [2]. A recently used method to capture the temperature of the whole bearing is the infrared thermography. The infrared thermography is the technique that allows (from the radiation emitted by a scene, of adapted equipments and techniques of mastery of the measure situation) to obtain the spatial and temporal distribution of the temperatures of this observed scene. In this study, the measuring of temperature based on infrared thermography allows us to detect the presence of abnormally warm zones on the surface of the bearing [3]. Problems with bearings are usually found by comparing the surface temperatures of similar bearings working under similar conditions. Overheating conditions appear as "hot spots", within an infrared image as usually found by comparing similar equipment [4].

Another method of detecting the fault is through analyzing the mechanical vibrations and transforming them into the Frequency-domain. Frequency-domain or spectral analysis of the vibration signal is perhaps the most widely used approach of bearing defect detection. The advent of modern fast Fourier transform (FFT) analyzers has made the job of obtaining narrowband spectra easier and more efficient. Both low and high frequency ranges of the vibration spectrum are of great interest, in assessing the condition of the bearing [5]. The interaction of defects in rolling element bearings produces pulses of very short duration whenever the defect strikes or is struck owing to the rotational motion of the system. These pulses excite the natural frequencies of bearing elements and housing structures, resulting in an increase in the vibrational energy at these high frequencies. The resonant frequencies of the individual bearing elements can be calculated theoretically. Each bearing element has a characteristic rotational frequency. With a defect on a particular bearing element, an increase in vibrational energy at this element's rotational frequency may occur. These characteristic defect frequencies can be calculated from kinematic considerations i.e., the geometry of the bearing and its rotational speed [6].

Apart from the measurement of mechanical vibration that caused by the machine, it is also measured the airborne acoustic ("air-borne sound"). Acoustic noise from mechanical vibrations produced within a machine from metallic components, lubricants, other moving objects or materials, from entrapped air or steam in the inner part of the machine. This noise in the air around the engine, called Air born sound. Measurement of acoustic noise can be used for the detection of defects in rolling element bearings [7].

2 Materials and Methods

2.1 Experimental Set-up

The instrumentation and experimental setup that was used for the needs of the present work is presented in Fig. 1.

The ball bearing that was used for charging was a common deep groove ball bearing with single mounting (type 6206 by Nachi). It was adapted in an axis and inside the load device (Fig. 1). The accelerometer was placed on the top of the load device. The bearing charged with a continuous radial load equal to 48,54 KN. The sensor signals were of altered tendency and with suitable conditioning circuitry leveled to the host computer, for storing and further processing with the LabView (National Instrument) program.

2.2 Applying Load on the Bearing

The load device for the applying of charge of the bearing was studied for both radial and axial stress. For radial stress, the surface growing tension is $\sigma_1 = 57.6 \text{ N/mm}^2$, while the yield point of steel St 37-2 is $R_e = 210 \text{ N/mm}^2$ (safety factor on the surface deformation = 3.6), while for axial the surface stress in the cap of the structure is equal to $\sigma_2 = 34.3 \text{ N/mm}^2$ ($E_2 = 728 \text{ mm}^2$) (safety factor on the surface deformation in the cap = 6.1) [2]. After studying the
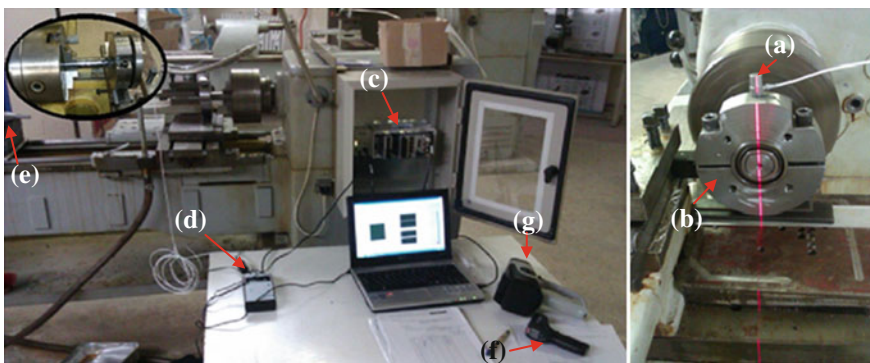

Fig. 1 Experimental setup: **a** One accelerometer (for vibration on the radial axis) (type 8702 B25 by Kistler), **b** A load device for the measurement of charge (constructed by a previous work in our laboratory (Fig.2) [2]), **c** A DAQ card for acquired data (type CompactDAQ—9172 by national instruments and the module NI 9233). **d** The coupling circuit for the accelerometer. **e** A microphone for the measurements of the acoustic emissions (Voltcraft Digital Schallpegelmass-gerat 329). **f** An Infrared thermometer (type KIRAY 100 by KIMO). **g** A portable thermal imager (type IVN 780-P by IMPAC)

Fig. 2 Steel construction
(Stall 37-2), with shear
modulus G equal to
80 KN/mm^2
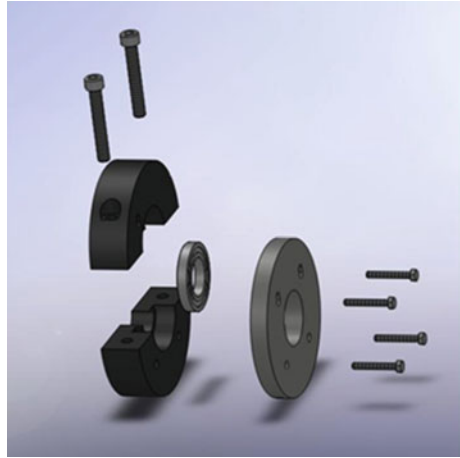
strain-machine, there had to be calculated the load of the bearings, caused by the screw, and therefore had to be calculated the torque from the torque wrench that were used on the two radial screws, by using the equations of Mann :

Friction by Mann: $M_{an} = M_G + M_A = F \times r_2 \times \tan(\alpha + \rho\prime) + F_{\mu A} \times r_A = 49.99$ Nm

where M_G, is the friction torque of the thread and M_A is the torque from the torque wrench, for F = 24.27 kN, $\rho\prime = 9$, $r_2 = d_2/2$, $\alpha = 2, 9^o$, $\mu_A = 0, 11$, $r_a = 0.7$ d, $d_2 = 10, 863$ mm.

The basic rating life of the bearing 6206 for radial load equals to 48.54 KN according to ISO 281:1990 is: $L_{10} = \left(\frac{C}{P}\right)^{P} = \mathbf{0.0731}$ or $L_{10h} = \frac{10^6}{60 \, n} L_{10} = 1.219$ h or 73.14 min. Nevertheless, the experiment lasted 110 min so that the fault could be easier detected.

2.3 Temperature and Infrared Thermography

The measuring of the rolling bearing temperature has been done with the infrared thermometer (Fig. 3). After analyzing the increasing temperature, further details had to be added in order to specify which parts of the bearing exactly did the fault occurred. At this point were used the method of Infrared thermography. The thermographs were acquired by a fixed thermographic camera and were processed and recorded every 20 min. A study of machine tool spindle to obtain an assembly presenting a limited temperature increase at high speed monitored the fatigue life of bearings [8]. It showed by model and by experiment that a temperature rise between 16 and 34 °C was to be expected in normal working conditions. In the study of J.-S. and K.-W Chen, for bearing load for high speed spindle, it was clearly showed that the temperature of the bearing depend on the load and on the rotational speed [6].

Fig. 3 Infrared thermometer

2.4 Vibrations and Characteristic Frequencies

It is marked as mentioned before that, the vibrations width is an indicator of the vibration power and depends from the speed (Rpm) and the load (N) of the bearing. For a particular bearing geometry, inner raceway, outer raceway and rolling element faults generate vibration spectra with unique frequency components. It is these unique frequency components and their magnitudes that make it possible to determine the condition of the bearing. The bearing defect frequencies are linear functions of the running speed of the motor. Outer race and Inner race frequencies are also linear functions of the number of balls in the bearing. For a bearing, with the outer ring stationary, bearing key frequencies are calculated as follows (1–4) [9]:

$$\text{Fundamental Train Frequency (FTF)}: \quad f = \frac{f_s}{2 \cdot} \left(1 - \frac{B_d}{P_d} \cos \phi \right) \tag{1}$$

$$\text{Inner Race Frequency (IR)}: \quad f_i = Z(f_s - FTF) \tag{2}$$

$$\text{Ball spin frequency (BS)}: \quad f_b = \frac{P_d \, f_s}{B_d 2 \cdot} \left[1 - \left(\frac{B_d}{P_d} \right)^2 \cos \phi \right] \tag{3}$$

$$\text{Outer Race Frequency (OR)}: \quad f_o = Z(FTF) \tag{4}$$

where fs, Bd, Pd, φ and Z are the revolutions per second of the IR or the shaft, the ball diameter, the pitch diameter, the contact angle and the number of balls, respectively (Fig. 4). The contact angle for the ball bearings carrying no thrust load is assumed to be zero.

By the above equations it is calculated the defected frequencies for the bearing of this experiment. While knowing that is turning in the machine-tool of system with speed of 1,000 Rpm with $\cos\varphi = 1$, Bd = 10.40 mm, Pd = 47, 25 mm and Z = 9, the defected frequencies are: FTF = 58.49 Hz, IR = 91, 51 Hz, BS = 36, 03 Hz, and OR = 6.5 Hz.

Fig. 4 Deep groove ball
bearing
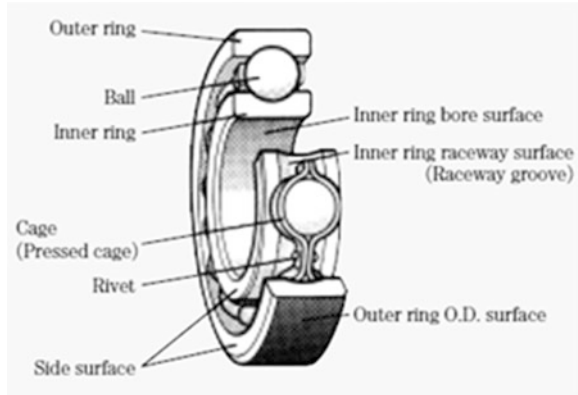
The ball bearing, as all the machine elements have a characteristic natural frequency vibration, while at the same time the frequencies with which their components are vibrating can be calculated, as the exterior ring, the internal ring or their balls. With the Fourier Transformation there can be distinguished the frequencies of ball bearing's elements and conceive if there is any damage in the particular component, so that the fault of the bearing can be averted. The principal advantage of the method is that the repetitive nature of the vibration signals is clearly displaced as peaks in the frequency spectrum at the frequency where the repetition takes place [10]. The FFT was applied on the signal acquired by LabView on the software environment of MatLab.

2.5 Air-Borne Sound

In this paper the air-borne sound were measured by the portable microphone (Fig. 5).

The microphone is a sensor that converts sound pressure into an electrical signal. Of great importance is how to load the microphone right. It should be placed always in the same place as the previous measurements so that the results

Fig. 5 Portable microphone

are comparable. The microphone should be placed at a distance greater than twice the length of the machine but not too far away from it as the received signal will permeate other sounds.

3 Results and Discussion

3.1 Temperature and Infrared Thermography

In Fig. 6, it is presented the evolution of temperature over time measuring by the portable thermometer.
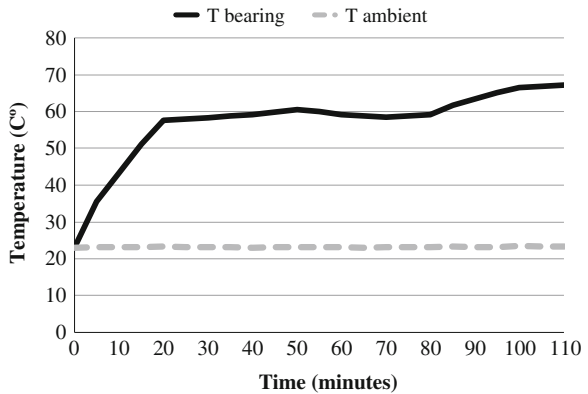
It is shown that at the beginning of the operation (the first 20 min) there was a high increase of the temperature. A steady low increasing temperature followed and at the end of the experiment a further increase had occurred depicting the fault of the bearing. Those temperatures were above the limit of normal working conditions of the bearing that is around 60 °C [11].

In the experiments that were conducted for the purpose of this paper there where depicted faults in two parts of the bearing, by the portable thermal imager. On the Fig. 7, it is shown that there was a hot spot with max temperature of 69.5 °C on one part of the outer ring, while the rest parts temperature were about 26 °C below.

The other part that an increased temperature was occurred is on the rolling elements (the balls), shown by Fig. 8.

At the Fig. 8 the numbers (1–9), represent the nine balls of the bearing, and at the ball number 3 there was an increased temperature, about 5 °C more than the others, declining a fault at this ball.

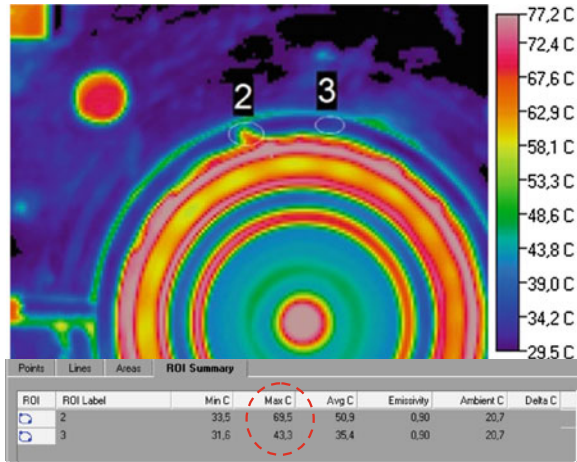**Fig. 6** The evolution of temperature over time diagram

ROI	ROI Label	Min C	Max C	Avg C	Emissivity	Ambient C	Delta C
	2	33,5	69,5	50,9	0,90	20,7	
	3	31,6	43,3	35,4	0,90	20,7	

Fig. 7 Thermal image depicting a hot spot on the outer raceway

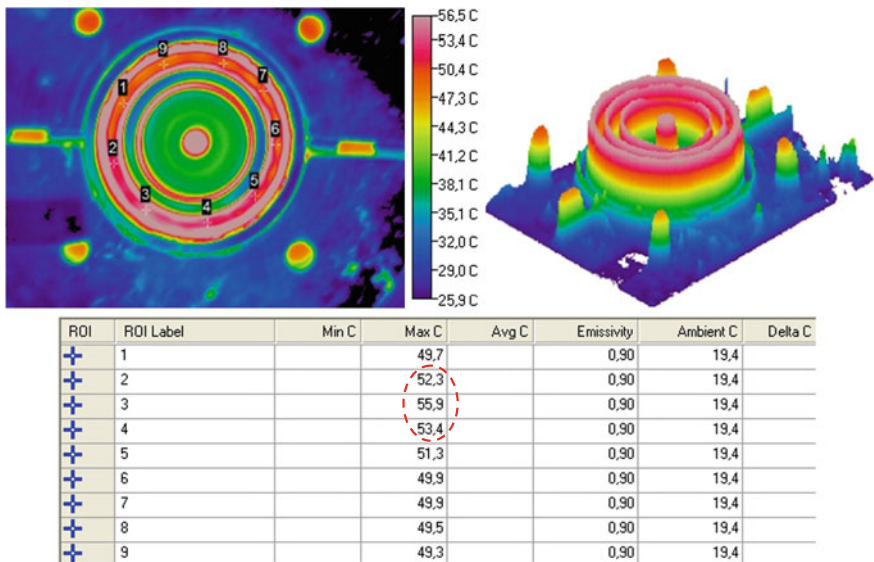| ROI	ROI Label	Min C	Max C	Avg C	Emissivity	Ambient C	Delta C
+	1		49,7		0,90	19,4	
+	2		52,3		0,90	19,4	
+	3		55,9		0,90	19,4	
+	4		53,4		0,90	19,4	
+	5		51,3		0,90	19,4	
+	6		49,9		0,90	19,4	
+	7		49,9		0,90	19,4	
+	8		49,5		0,90	19,4	
+	9		49,3		0,90	19,4	

Fig. 8 Thermal image depicting a difference of temperature in the balls of the bearing and also the 3-D profile of it

3.2 Vibration Analysis-FFT

The analysis of the signal by the use of the FFT is presented on the Fig. 9.

It is depicted the appearance of fault in various part of the rolling element, defined by the appearance of the characteristic frequencies and their harmonics.
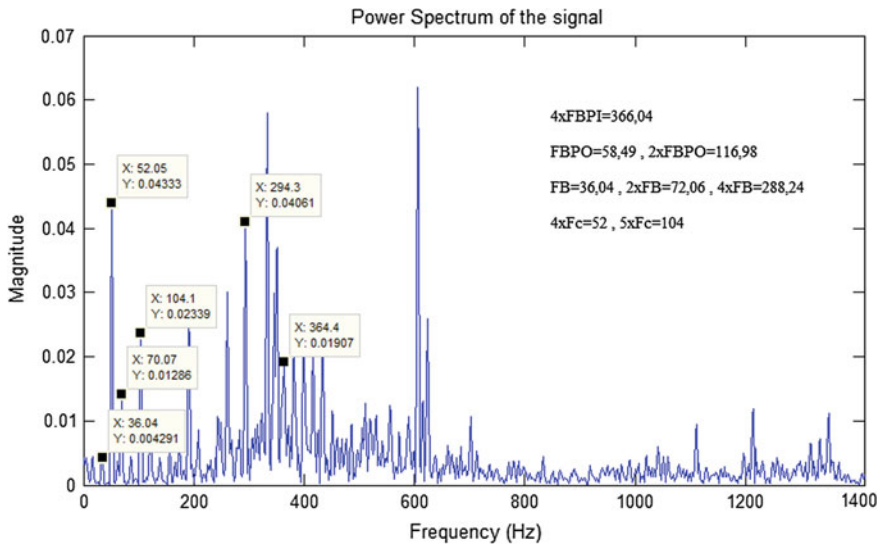
Fig. 9 The extracted plot from MatLab with the characteristics frequencies

More precisely, on the plot it is visible the first second and forth harmonics of the FB (FB = frequency when one point on a rolling element is damaged), declining fault on the rolling elements (the balls). Also the first and second harmonics of the FBPO (FBPO = frequency when one point on outer raceway is damaged), showing the fault on the outer raceway of the bearing. Some fault can also be seen at the parts of the cage (Fc) (fourth and fifth harmonics) and at the inner raceway (fourth harmonic).

3.3 Cost Analysis

At this point, a comparison of the cost between thermography and vibration analysis was also vital in order to compare those two methods on a more large scale view. The Table 1 depicts the total cost of each method respectively for the equipment they occurred. It is shown that the method of thermography is cheaper than the one of the vibration analysis.

Table 1 Total cost of vibration analysis and thermography equipment

Method	Used equipment					Total cost
Vibration analysis	Accelerometer	Software	Coupling circuit	DAQ— 9172	Work hours	7,000–9,000 euro
Thermography	Thermal imager	Software	Work hours			5,000–7,000 euro

Fig. 10 The sound pressure evolution over time during the experiment
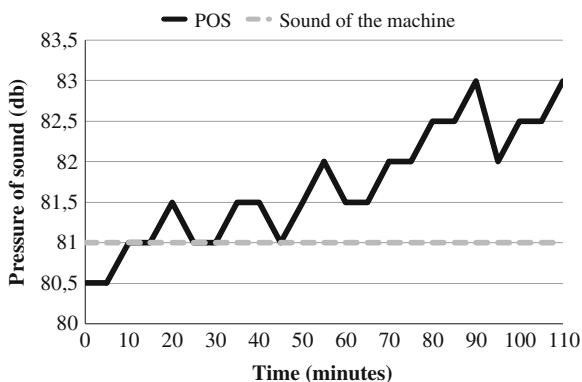
3.4 Air-Borne Sound

In the Fig. 10, it is presented the sound pressure evolution over the time of the conducted experiment. It is shown that over the time there was an increase of the sound pressure depicting extensive use of the machine as well increased stressing of the bearing element.

4 Conclusions

In this paper, a comparative analysis had been used, by applying three methods. The results had shown that the data acquired by the analyzed thermal images, the signal processing from the accelerometers and the rising levels of the air born sound are all relevant between them. The vibration analysis is the most common and precisely method of detecting fault on bearings but still it's a method requiring well trained staff and greater time and money for the acquisition of the results. So the results are depicting that even if the vibration analysis is the most common method of detecting fault on bearings, it still can be replaced by the use of other methods less accurate but less difficult to operate. Further testing under variable and/or axial loads is under investigation by the present research team before a final conclusion can be made. The finite element analysis will be also examined, as promising method of detecting the fault on bearings.

References

1. Tandon N, Choudhury A (1999) A review of vibration and acoustic measurement methods for the detection of defects in rolling element bearings
2. Rodopoulos K (2009) Design, study and construction of module for stress on bearings. Thesis presented on DUTH University

3. Maldague XPV (2001) Theory and practice of infrared technology for nondestructive testing. Wiley, New York
4. Leemans V, Destain M, Kilundu B, Dehombreux P (2011) Evaluation of the performance of infrared thermography for on-line condition monitoring of rotating machines
5. Mouroutsos SG, Chatzisavvas I (2009) Study and construction of an apparatus that automatically monitors vibration and wears in radial ball bearings which are loaded in radial direction. 2009 International conference on signal processing systems, IEEE computer society, pp 292–296
6. Chen J-S, Chen K-W (2005) Bearing load analysis and control of a motorized high speed spindle. Mach Tools Manuf 45(12–13):1487–1493
7. Tandon N, Choudhury A (1999) A review of vibration and acoustic measurement methods for the detection of defects in rolling element bearings. Tribol Int 32:8
8. Jiang A, Mao H (2010) Investigation of variable optimum preload for a machine tool spindle. Int J Mach Tools Manuf 50(1):19–28
9. Ocak Hasan, Loparo KA (2004) Estimation of the running speed and bearing defect frequencies of an induction motor from vibration data. Int J Mech Syst Sig Process 18:515–533
10. Botsaris PN, Koulouriotis DE (2007) A preliminary estimation of analysis methods of vibration signals at fault diagnosis in ball bearing. 4th International conference on NDT, Chania
11. Detweiler WH (2011) Common causes and cures for roller bearing overheating. SKF USA Inc., King of Prussia, PA